Presented at the 35th European PV Solar Energy Conference and Exhibition, 24-28 September 2018, Brussels, Belgium

NANOINDENTATION ANALYSIS OF PV MODULE POLYMERIC COMPONENTS AFTER ACCELERATED AGING

Djamel E. Mansour[1], Fabian Swientek[2], Ismail Kaaya[1], Daniel Philipp[1], Luciana Pitta Bauermann[1]
1 Fraunhofer Institute for Solar Energy Systems ISE
Heidenhofstrasse 2, 79110 Freiburg im Breisgau, Germany
+49-761-4588-5880
2 Anton Paar Germany GmbH
Helmuth-Hirth-Str. 6, 73760 Ostfildern, Germany
Djamel.eddine.mansour@ise.fraunhofer.de
https://www.ise.fraunhofer.de

ABSTRACT: The degradation and failure of a PV module can be caused by mechanical property changes in the polymeric components during its lifetime. Previously most of the investigation of the mechanical changes, for example hardness, as well as the aging has been carried out with the polymeric materials as bulk. With nanoindentation the change in hardness of encapsulant and backsheet can be spatially resolved with a high lateral resolution. The nanoindentation tests were carried out on the cross-section of glass/encapsulant/backsheet laminates after sequential doses of 500 h damp-heat (DH) at 85 °C and 85 % r.h. Backsheets with different water vapor permeation rates were used. The results show an increase in hardness (up to 40 MPa from 500 h to 2000 h DH) for the PET-based backsheet (BS1) with the highest water vapor permeation rate, which suggests a high degree of hydrolysis of the PET core layer. The hardness values of the encapsulant in the PV laminate showed a uniform increase with a slightly depth-dependence after DH aging. Especially after 500 h DH exposure, the hardness values were slightly higher near the BSF/encapsulant interface.

Keywords: encapsulant, backsheet, damp-heat (DH) exposure, degradation, nanoindentation, hardness, water vapor permeation, hydrolysis.

1 INTRODUCTION

The lifetime of a PV module is generally limited by the degradation of the constituent parts. The polymeric materials - encapsulants and backsheets - are particularly susceptible to degradation influencing the PV module's long-term reliability. These components are essential for mechanical protection and electrical insulation. When PV modules are exposed to environmental conditions like heat, humidity and UV irradiance, they suffer chemical degradation, triggered by a complex interaction of different aging mechanisms [1]. An increased level of moisture content in polymers leads to loss of molecular weight, loss of adhesion, loss of electrical insulation properties, and higher vulnerability to mechanical failure. Moisture can diffuse into PV modules through the permeable backsheets and the encapsulant layers towards the solar cell weakening their interfacial adhesive bonds, resulting in delamination and an increased number of ingress paths [2]. A deeper understanding of this process is of high importance for a better reliability and durability of PV modules [3].

Numerous attempts have been made to estimate water concentration in encapsulants using gravimetric methods [4] and water vapor transmission rate measurements [5]. However, the influence of the mechanical properties of encapsulants inside the PV module has not been thoroughly investigated. There is still a missing link between the aging process and its consequences in the context of mechanical properties [6]. The stability of the encapsulant aged in damp-heat (DH) has been investigated by using this material as granules [7] and free standing films [4]. The hydrolytic stability of polyethylene terephthalate (PET) bulk, a common core layer of PV backsheets (BS), has been studied at different temperatures and different relative humidities (RH) [8]. The degradation of adhesion strength between the backsheet and encapsulant due to moisture penetration was investigated for crystalline silicon photovoltaic mini-modules. The adhesion strength was measured by 90° peel tests, carried out at specified time intervals during accelerated aging tests [9]. The adhesion decreases quickly at the beginning and stabilizes after a certain time. An increased humidity accelerates the loss of adhesion. The thermo-viscoelastic properties of the encapsulant play an important role for adhesion, since the Young's modulus expressing the adhesive stiffness is strongly temperature-dependent [10].

This paper summarizes the research result on the change in hardness occurred in the encapsulant and PET-based BSs under DH conditions. The encapsulant was laminated between glass and different backsheets. The use of a backsheet allows entrance of humidity in an order of magnitude comparable to state of the art PV modules. The aging of the encapsulant in a PV module-like design is very important, because the water vapor diffusion, solubility and accumulation may differ on its

bulk or on the interfaces. The object of this research is to identify the mechanical/hardness properties changes along the thickness of the BS and encapsulant. For this purpose, the chosen methodology is nanoindentation, as it allows measuring the hardness of the materials with a high spatial resolution.

To the best of our knowledge, the nanoindentation is a new destructive technique for mechanical testing of the PV module components after accelerated aging. In this way the effect of the hydrolysis as well as the oxidation of the polymers can be measured and localized from the external backsheet surface throughout the encapsulant to the glass.

2 EXPERIMENTAL PART

2.1 Lamination of the samples

PV laminates (18 x 18 cm^2) were prepared by laminating a layer of backsheets (BS), 2 layers of ethylene-vinyl acetate (EVA) as encapsulant and a non-tempered transparent glass cover (Fig. 1). The backsheet foils both have PET as core layer and water vapor permeation values reported for different temperatures on to their datasheets: BS1 = 3.9 g/m²·d at 38°C / 90% r.h, BS2 = 0.7 g/m²·d at 23 °C / 85% r.h.

2.2 Accelerated aging

The laminates were exposed to high humidity and temperature. The conditions of the damp-heat (DH) tests were 85 °C and 85 % r.h. during time intervals of 500 h. The accelerated aging test was based on the International Electrotechnical Commission (IEC) standard "IEC61215: Terrestrial photovoltaic (PV) modules–design qualification and type approval" [11].

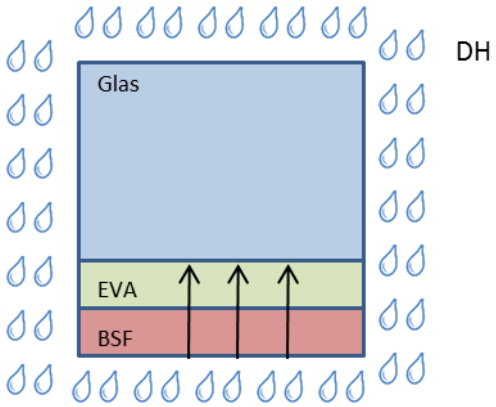

Figure 1: Schematic illustration of the laminate during accelerated aging

2.3 Cross-section sample preparation

The cross-section of the laminate was prepared after the accelerated aging by using a glass cutter to cut the glass followed by a sharp scalpel to cut the polymer layers. The cross-sections were extracted at a distance of at least 3 cm from the edge, to avoid effects from lateral humidity transmission. The piece of laminate was embedded in epoxy resin and polished with polycrystalline diamond suspension (Fig.2).

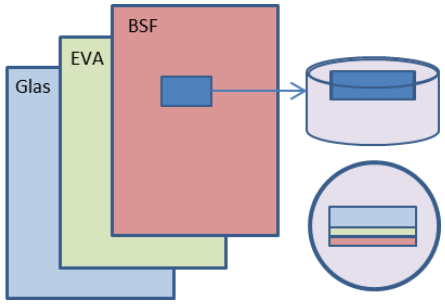

Figure 2: Schematic illustration of the cross-section preparation for the nanoindentation

2.4 Nanoindentation testing

All experiments were performed using the Nano Hardness Tester NHT^3 from Anton Paar Company. The system has load and displacement resolution of up to 500 mN and 200 µm respectively. The three-side pyramid with an area-to-depth function similar to a Vickers diamond indenter geometry, was used in all experiments as shown in Fig. 3. Based on Oliver and Pharr [12] the hardness (H) is defined as the pressure the material will support under load and is calculated from the peak indentation load (P_{max}) divided by the projected area (A) according to :

$$H = \frac{P_{max}}{A} \qquad \text{eq 1.}$$

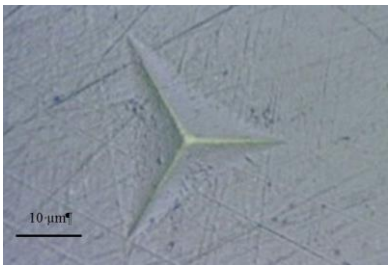

Figure 3: Microscopic image of the three-side pyramid indented on the PET-based backsheet

The indentations were performed at a distance of 44 µm between each point. The possible distance between the indentations is inversely proportional to its depth. A deeper indentation affects a larger area of the polymer and the distance between the measurements have to be large enough to avoid an overlapping.

3 RESULTS AND DISCUSSION

3.1. Ideal depth of nanoindentation

The hardness of the polished cross-sectional material might be affected by the sample preparation. In order to

have a coherent value of hardness of the polymers and remove the influence of the exposed surface, a pre-measurement was conducted to find the ideal depth of the nanoindentation tip. A load is applied until the hardness value stays constant. The values of maximum load were fixed at 50 mN for BS and 100 mN for EVA.

A typical graph of load versus indenter displacement used for the calculation of hardness of BS and EVA is shown in Fig.4. For similar load (ca. 50 mN) the indenter in the BS (3,500 nm) is much shallower than in the EVA (30,000 nm). The hardness is calculated from eq. 1 by maintaining the load constant and measuring the indenter displacement or the indented area left after the unloading of the indenter.

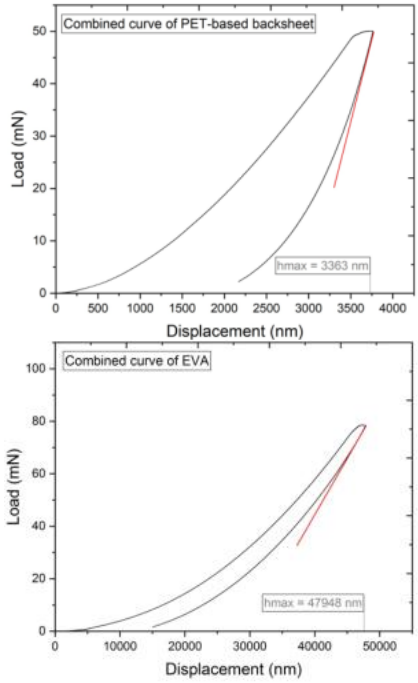

Figure 4: Combined curves of load versus indenter displacement used for the calculation of hardness of BS (top) and EVA (bottom)

3.2 Changes in hardness of BS during DH aging

The laminates were aged for 4 intervals of 500 h DH each. The hardness was measured after each interval. Fig.5 shows the deformations left on the BS surface after the indentations.

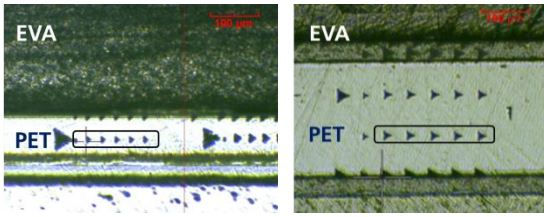

Figure 5: Microscopic images of the cross-section of the laminates after indentations on the BS1 (left) and BS2 (right) as laminated in glass/EVA/BS stack and aged under DH conditions. The values of the five indents on the same plane are averaged.

In this work the hardness of the core layer of the BSs was calculated on the middle of the PET layer. The measurement of the hardness of two BSs at different aging steps is shown in Fig.6. Five indentations were performed on the each line parallel to the interfaces and an average value was calculated.

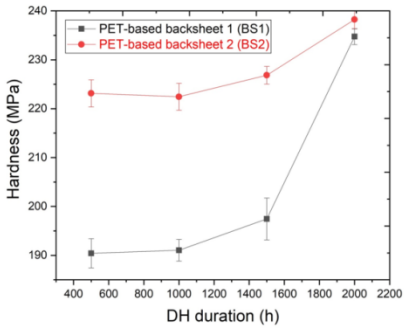

Figure 6: Changes in hardness of BSs after different intervals of DH aging

The initial hardness values of BS1 are lower than those of BS2, due to the difference of PETs. The change in hardness during the DH aging is much higher for the BS1 than for the BS2. This could be explained by the higher water vapor permeation rate of BS1, due to which the hydrolysis could happen to a higher extent. Or the PET-based BS2 is more stable.

3.3 Changes in hardness of EVA during DH aging

As the EVA is more elastic than BS, its deformation after the indentation is barely visible. The positions of the indentations are drawn as red triangles in Fig.7. The depth 1 is close to the BS and it is in contact with water vapor in the early stages of DH. The depths 2 and 3 are further in the interior of the EVA layer. Depth 4 is the furthest away from the BS and closest to the glass.

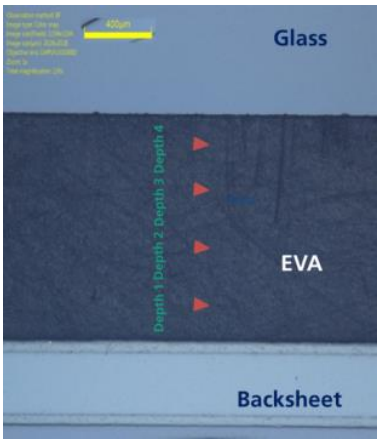

Figure 7: Microscopic images of the cross-section of the glass/EVA/BS laminate. Red triangles indicate the measurement points (depth) lateral from 1 (closest to backsheet) to 4 (closest to glass).

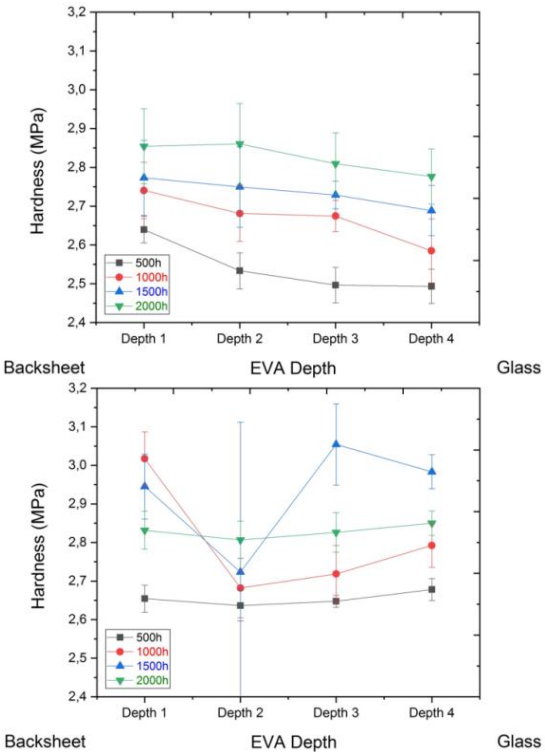

Figure 8: Changes in hardness along the thickness of the EVA laminated with BS1 (top) and BS2 (bottom) after different intervals of DH aging

According to Fig.8 (top) after 500 h DH, the EVA laminated with BS1 shows a stronger increase in hardness close to the BS than in the middle of the EVA or close to glass. After each DH interval, the EVA gets more homogeneous along its thickness and the hardness increases in general. The hardness of the EVA is slightly higher close to the BSF interface in all aged stages.

The laminate with BS2 (Fig.8, bottom) shows a homogeneous hardness along the EVA layer after 500 h and 2000 h DH. This hardness increases with the aging from 500 h DH to 2000 h DH. The hardness for the EVA aged after 1000 h DH and 1500 h DH show unexpected values. We suppose that the displaced EVA area through the indenter was very large and an overlapping between adjacent indenters happened invalidating the result. It might also be that the first point (at depth 1) was too close to the BS and the value was not correct due to the proximity of the interface.

4 CONCLUSION

In this work, nanoindentation was used as a suitable destructive method to investigate the changes in hardness occurred during DH aging of components in the PV modules with a high spatial resolution. The hardness of two different PET-based backsheets increased by prolonged DH exposure time, especially after 1500 h. The increase in hardness of BS1 (high water vapor permeation) was as expected higher than in BS2 (low water vapor permeation) due to a higher moisture ingress. The DH exposure induced a slight increase in the hardness values of the encapsulant. Using the BS1 in the PV laminate, the encapsulant shows an increase hardness values close to the interface BS/Encapsulant. The increase in hardness of BS and encapsulant may indicate an early stage of the PV degradation. Additional research is planned to identify a level of hardness where delamination is about to happen. These are the first results showing the possibility of measuring the change in hardness of the polymeric material of a PV module due to aging. Further work is being done to improve the quality of the measurements by better defining the position and depth of the indents. Also other characterization techniques are going to be used to complement and give stronger arguments for our conclusions. In the future, degradation models will be used to extract the kinetic parameters and correlate them with the different failure modes induced by the accelerated aging tests.

5 ACKNOWLEDGEMENTS

We would like to express our gratitude to Paul Pavlov and his team in Anton Paar Germany GmbH Company for providing much expertise on the Nanoindentation. This work has been funded by the European Union's Horizon 2020 programme under the Marie Sklodowska Curie Actions GA No. 721452, acronym SOLAR-TRAIN.

References

[1] A. Badiee, I.A. Ashcroft, R.D. Wildman; International Journal of Adhesion and Adhesives 68 (2016) 212
[2] N. Park, C. Han, and D. Kim, Microelectron. Reliab., 53 (2013) 1922
[3] R. Meitzner and S.-H. Schulze, Sol. Energy Mater. Sol. Cells, 144 (2016) 23
[4] T. Swonke, and R. Auer, Proceedings .SPIE, (2009) 74120A-1
[5] S. Rashtchi, P. D. Ruiz, R. Wildman, and I. Ashcroft, Proceedings SPIE 8472 Reliability of Photovoltaic Cells, Modules, Components, and Systems V, (2012), 847200)
[6] D. Wu, J. Zhu, T.R. Betts, R. Gottschalg. Prog Photovoltaics Res Appl, 22 (2014) 796
[7] M. Çopuroğlu, M. Şen Polym. Adv. Tech. 15 (2004) 393
[8] James E. Pickett, Dennis J. Coyle. 98 (2013) 1311
[9] D. Wu, J. Zhu, T.R. Betts, R. Gottschalg. Prog Photovoltaics Res Appl; 22 (2014) 796
[10] M. Köntges, G. Oreski, U. Jahn, M. Herz, P. Hacke, K. A Weiss IEA PVPS (2017)
[11] ICE 61215, Terrestrial photovoltaic (PV) modules-Design qualification and type approval, International Electrotechnical Commission, (2016)
[12] W. C. Oliver, G. M. Pharr, J. Mater. Res., 6 (1992) 1564